applied sciences

MDPI

Article

Impact of Part Positioning along Chamber Z-Axis and Processing Parameters in Selective Laser Sintering on Polyamide Properties

Ana Pilipović *, Petar Ilinčić *, Mislav Tujmer and Maja Rujnić Havstad

University of Zagreb Faculty of Mechanical Engineering and Naval Architecture, Ivana Lučića 5, 10000 Zagreb, Croatia; mislav.tujmer@fsb.unizg.hr (M.T.); maja.rujnic@fsb.unizg.hr (M.R.H.)
* Correspondence: ana.pilipovic@fsb.unizg.hr (A.P.); petar.ilincic@fsb.unizg.hr (P.I.)

Featured Application: The application of the research results includes help in determining the influencing processing parameters when making products by selective laser sintering. It is known from previous research that energy density has the greatest influence, and, according to many equations given by other authors, the most important factor in energy density is the hatch distance (distance between the paths of the laser beam). Furthermore, due to the SLS technology working principle, to optimize printing costs, a complete working chamber should be used for printing as much as possible. Therefore, this study provides an insight into whether the same mechanical properties and dimensional stability are achieved if 3D-printed parts are processed with different processing parameters at different heights of the working chamber with respect to the *z* axis.

Abstract: Additive manufacturing procedures are being increasingly developed, from prototyping to finished functional products. However, their rapid development also brings along the testing of properties with different manufacturing parameters. In selective laser sintering, the most influential manufacturing parameter is the energy density, which also consists, among other things, of the hatch distance. For better usage of the entire chamber and a reduction in the overall price of the finished product, in practice, the manufacturing of products at different heights (levels) of the working chamber with different orientations is inevitable. The study examines how hatch distance and product orientation impact the tensile strength and dimensional stability of polyamide products across two levels within the chamber. Upon analysis, it was observed that manufacturing products at different levels within the working chamber does not influence their dimensions. Achieving precise product dimensions comparable to those in the CAD model is possible. Furthermore, the same factors (orientation and hatch distance) and their combinations affect the length, thickness, and width of the product. Although all test specimens were tested, a tensile strength analysis of variance (ANOVA) of test specimens produced at the lower level of the chamber with a combination of hatch distance (ranging from 0.23 to 0.6 mm) and orientation (ranging from 0° to 60°) was not feasible in the design of the experiment. Despite this limitation, it was noted that both chamber levels had the potential to reach a maximum tensile strength of 47 N/mm^2. Nevertheless, the average tensile strength of PA12, obtained through combinations of input factors, stood at only 30 N/mm^2, which is quite a low value for polyamide made by selective laser sintering.

Keywords: dimensional stability; hatch distance; mathematical model; orientation; polyamide PA12; response surface; selective laser sintering—SLS; tensile strength; working chamber levels

Citation: Pilipović, A.; Ilinčić, P.; Tujmer, M.; Rujnić Havstad, M. Impact of Part Positioning along Chamber Z-Axis and Processing Parameters in Selective Laser Sintering on Polyamide Properties. *Appl. Sci.* **2024**, *14*, 976. https://doi.org/10.3390/app14030976

Academic Editor: Arkadiusz Gola

Received: 2 January 2024
Revised: 21 January 2024
Accepted: 22 January 2024
Published: 23 January 2024

1. Introduction

In selective laser sintering (SLS), the laser beam energy softens the powder material, resulting in the sintering of particles and the fusion of the newly applied layer with the previously sintered [1–3].

During this process, the laser beam must simultaneously melt new powder particles in the next layer and sinter this current layer with the already existing one. The possibility

of using various materials with different thermal conductivity as well as diverse layer thicknesses requires adequate energy input (energy density (ED)) to sinter the material at all and to unite this material layer with the previous. The laser beam melts a slightly thicker layer of powder every time in every layer, which results in a decrease in powder volume. To avoid excessive sintering, appropriate power must be set according to layer thickness. After the printing process is completed, several protective layers of powder (about 5 mm) are applied. For gradual cooling, the finished product is first left in the working chamber for about 2 h, after which it is removed from the chamber and left in powder outside the machine to cool to room temperature. Such a procedure maintains dimensional accuracy and avoids thermal deformation of the product. The cooling of the product usually takes as long as the production does. After the product has cooled to room temperature, it can be taken out of the unsintered powder and cleaned [3,4].

Energy density depends on the power and speed of the laser and on the hatch distance or on the laser beam diameter [1,4–9].

The value of laser power during the sintering depends on the material and the thickness of the layer. Laser power and speed can be different for the contour and hatching, and changing these parameters changes energy input and manufacturing time [1,4,7,8].

The accuracy of all additive manufacturing processes depends on how the product is positioned along the *x*-*y*-*z* axis within the chamber. Product resolution, product surface, and manufacturing time depend on product orientation in the working chamber, particularly if the product is manufactured with a large layer thickness (>0.25 mm) and if the material features strong anisotropy. A big drawback of additive manufacturing is the repeatability of accuracy and mechanical properties. The tolerances of dimensions cannot be determined in advance since they depend on material and many processing parameters [10].

Polymerization leads to an increase in the material density and percentage of shrinkage of the product. Therefore, it is necessary to enlarge the product to a different percentage in the *x*, *y*, and *z* axes to compensate for shrinkage that occurs after hardening and/or cooling. It is extremely difficult to determine the percentage of shrinkage since it requires careful calculation and experience, and for every product, the procedure is different [10].

Final products can be produced in SLS, and therefore the products must have high dimensional accuracy. But they are affected not only by converting the model into STL format and cutting the layers (certain layer thickness), but also by the resolution of the 3D printer, shrinkage of the used material, speed, power, hatch distance, and processing temperature. But one of the biggest causes of the inaccuracy of the product is the shrinkage of the material, which is different in different directions (*x*, *y*, and *z* directions). Shrinkage is also increased by sintering at higher temperatures, as in the case of thin-walled products. During crystallization, the molecules arrange themselves so that they occupy smaller volumes, which leads to material shrinkage [5,11,12].

In the experiment [10], it was observed that the parameters exhibit interdependence, alongside additional factors impacting the mechanical properties of the product. Thus, energy density must be calculated by the equation, which consists of the beam overlay ratio *x*, which includes the hatch distance and laser beam diameter:

$$ED = \frac{P}{v \cdot HD} \cdot x \tag{1}$$

where ED [J/mm^2]—energy density, HD [mm]—hatch distance, v [mm/s]—laser beam speed, P [W]—laser power, and x—beam overlay ratio, which is calculated according to the following:

$$x = \frac{d}{HD} \tag{2}$$

where d [mm]—laser beam diameter, HD [mm]—hatch distance. On the *Formiga P100* (manufactured by EOS GmbH—Electro Optical Systems, Krailling, Germany) machine where measurements were conducted, d is constant (d = 0.42 mm).

Numerous factors in SLS affect mechanical, thermal, and rheological properties, roughness, and dimensional stability. Some parameters, like laser power, hatch distance, laser diameter, and scan speed, which are all combined by Equation (1) into energy density, are widely regarded by many authors as the most important in this context.

Because of the orthogonal trajectories of the laser beam during exposure, different orientations of the samples in the *xy* direction may lead to different mechanical properties. Thus, Stoia et al. [13] found that the orientations of 0°, 30°, 45°, and 90° do not significantly affect the tensile strength.

The influence of orientation, power, and hatch distance on tensile strength showed that changing the orientation in the *xy* axis of the test specimens by 45° and 90° relative to 0° resulted in decreased values. However, when the laser power was at its peak, values around 27 MPa were achieved [14].

Wörz et al. investigated various hatch strategies and found that alternately hatched specimens showed an increase in tensile strength. A maximum tensile strength of 50 N/mm^2 was achieved [15].

According to the given Equation (1), Lopes et al. found that varying energy densities impact the tensile properties of polyamide 12 made by selective laser sintering. Results from tensile testing show that the implementation of a skin/core configuration allows the production of SLS parts with a valuable set of properties, minimizing the trade-off between mechanical strength and overall accuracy [16].

Furthermore, it is necessary to highlight the work of Razaviye et al., in which they determined the influence of processing parameters (laser power, scan speed, hatch distance, and scan length) on key mechanical properties (strength, modulus of elasticity, and elongation) of PA12 printed parts using the response surface methodology. The results showed that hatch distance is a major influencing factor in mechanical properties [17].

In our practice, it has been shown that when making products at different levels in the working chamber (looking at the height along the *z* axis) with selective laser sintering, deviations in dimensions occur, and when working at higher levels, the deviations are higher. Accordingly, the research in this paper is focused on the comparison of dimensions at different levels in the chamber through statistical analysis in the software Design Expert ver.13 (Manufacturer Stat-Ease, Minneapolis, MN, USA). There are not many works that compare the dimensions at various levels along the *z* axis in the working chamber, because most often they try to reduce costs, and due to the very logic of laser sintering in the SLS process, the chamber is filled along the *x* and *y* axes and then in the *z* axis. Furthermore, in accordance with the reviewed literature, hatch distance is the most influential parameter in the total energy density, and it was taken along with orientation as input parameters in both levels. In addition to the dimensions, the influence of the mentioned parameters in the upper and lower parts of the working chamber on the tensile strength was also tested.

2. Materials and Methods

The central composite plan has been selected for the experiment, which allows modeling of the polynomial of the second order and the shape of the response surface. From everything described in the Introduction, it can be concluded that the hatch distance has a significant influence on the selection of the parameters in the energy density (Equations (1) and (2)). Consequently, in subsequent research, it has been chosen as one of the parameters for assessing tensile strength and dimensions. The product orientation has been selected as the second parameter, and the test specimens have been set at two heights (levels) in the working chamber, as shown in Figure 1.

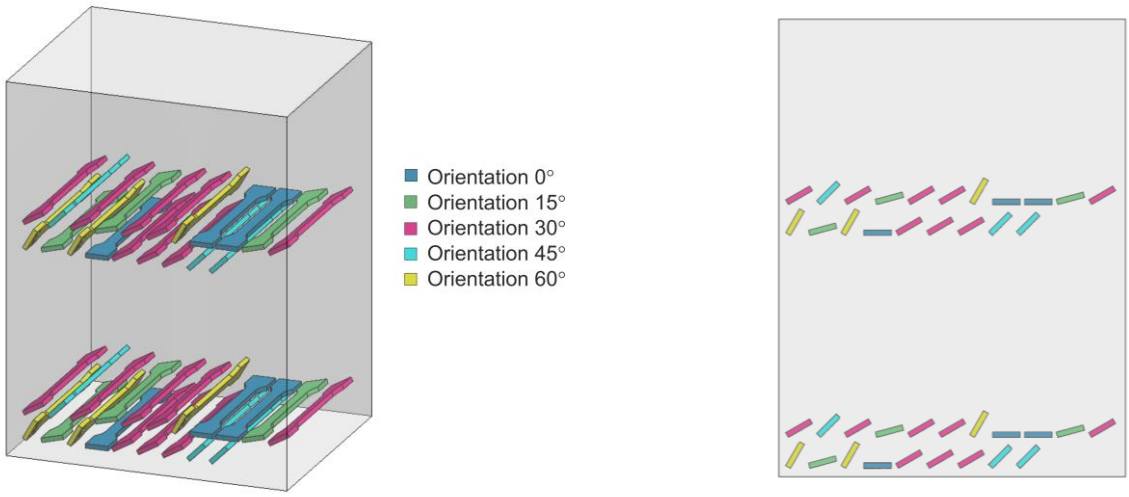

(**a**) (**b**)

Figure 1. Orientation of the test specimen in the machine working area: (**a**) production plan in a 3D printer—isometry; (**b**) production plan in a 3D printer—front view.

Manufacturing of the initial test specimens started at a height of 6 mm relative to the working platform (first level) and finished at 48 mm. The second level began at 174 mm from the working platform and finished at 216 mm.

Such a configuration of test specimens was printed in 3 separate print jobs to check the reproducibility of the results.

The tensile properties of thermoplastics are determined according to the HRN EN ISO 527:2019 standard [18]. The standard defines the equations to calculate the tensile properties and the dimensions of the test specimen. The tensile properties are tested with *Messphysik Beta 50-5* (manufactured by Messphysik Materials Testing, Fürstenfeld, Austria) with a max force of 50 kN and with a video-extensometer (Figure 2). Tests were carried out at room temperature (23 °C) at a speed of v = 5 mm/min. The test was carried out on 3 test specimens, and then the mean value and standard deviation were calculated.

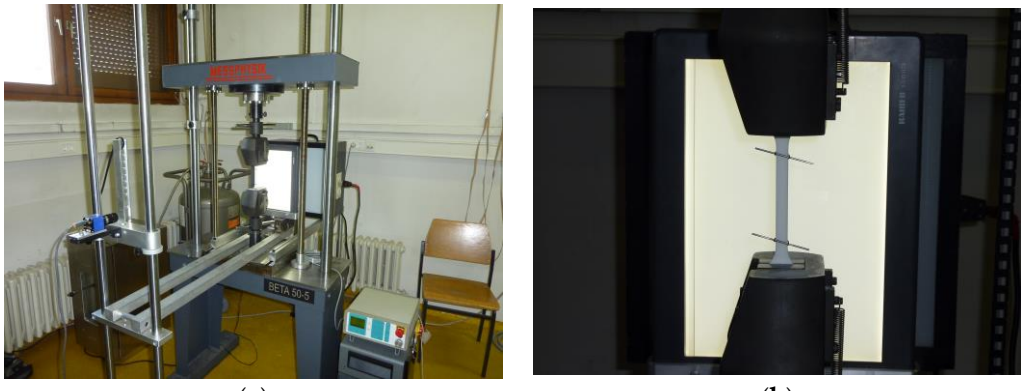

(**a**) (**b**)

Figure 2. Testing of tensile properties: (**a**) universal testing machine *Messphysik Beta 50-5*; (**b**) testing the test specimen.

When examining dimensional stability, three dimensions of the test specimen were considered, aligning with the standards set for the dimensions of the tensile test specimens:

- overall length $l = 150 \pm 2$ mm;
- thickness $h = 4 \pm 0.2$ mm;
- width $b = 10 \pm 0.2$ mm.

The dimensions were measured by a TMA MEBA caliper.

Software DesignExpert ver. 13 with the module ANOVA (analysis of variance) was used. In the work, the response surface method was applied with a user-defined experiment design. The reason for applying the user-defined experiment design was to obtain the precisely determined values of the orientation parameter within the limits of 0–60° with steps of 15°.

The data were processed by the ANOVA (analysis of variance) module.

The experiments were performed with the material polyamide 12 (PA 12) in Formiga P100 from producer EOS GmbH—Electro Optical Systems, Krailling, Germany (Figure 3), with the following other processing parameters:

- Building strategy sorted;
- Laser power to make the contour: 16 W;
- Laser beam speed for making the contour: 1500 mm/s;
- Laser power for making the hatching: 21 W;
- Laser beam speed for making the hatching: 2500 mm/s;
- Production temperature in the working chamber: 168 °C.

Figure 3. *Formiga P100*, a 3D printer on which test specimens are made.

3. Results

Before the test, a pre-experiment (preliminary test) was performed to determine the lower and upper limits of the factor (outside these limits, the preliminary test showed that the test specimens have poor quality):

A—hatch distance, *HD* = 0.23 to 0.6 mm;

B—orientation of the test specimen in the machine manufacturing area, $\alpha = 0^\circ$ to 60°.

Figure 4 shows the test specimens made with the minimal and maximal hatch distance and position/orientation of 0°.

Table 1 shows the actual and coded values of the experiment factors for the tested area.

It was necessary to perform 20 experiment runs (the run in the center was repeated three times). The levels of factors were determined according to the matrix of experiment runs for the user-defined experiment design with two factors.

Three test specimens were manufactured for each of the 20 experiment runs involving orientation and hatch distance, situated across two levels within the working chamber of the machine. Subsequently, these specimens underwent testing for tensile strength. The mean value and standard deviation were calculated.

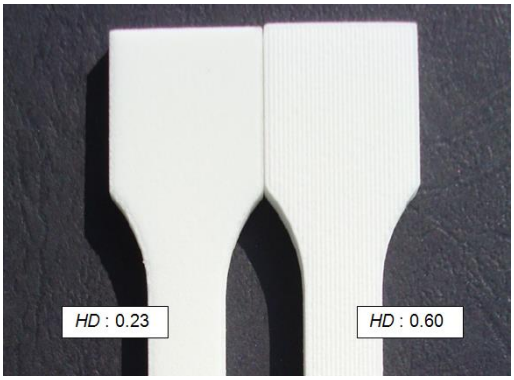

Figure 4. Test specimen with different hatch distances h = 0.23 mm (**left**) and h = 0.6 mm (**right**).

Table 1. Actual and coded values for experiment factors A and B.

Hatch Distance—A		Orientation—B	
Actual Values, mm	**Coded Values**	**Actual Values, °**	**Coded Values**
0.23	−1	0	−1
0.32	−0.5	15	−0.5
0.42	0	30	0
0.51	0.5	45	0.5
0.6	1	60	1

For each result, R^2 was determined, which is the measure of deviation from the arithmetic mean explained by the model. The closer R^2 is to 1, the better the model follows the data [19]:

$$R^2 = 1 - \frac{SSD_{residual}}{SSD_{model} + SSD_{residual}} \quad (3)$$

where R^2—R-squared, and SSD—sum of square deflection.

3.1. Results for Dimensions and Tensile Strength for the Upper Level of the Working Chamber

Table 2 shows the arithmetic means and standard deviations of tensile strength and dimensions (length, width, and thickness) of the upper level of the working chamber.

3.1.1. Results for Tensile Strength in the Upper Level of the Working Chamber

Table 3 shows the results of tensile strength at the upper level of the working chamber. One may conclude from the table that the hatch distance and the orientation of the test specimens have an almost equal impact on the tensile strength of the polyamide product. Factors A, B, AB, A^2, B^2, A^2B, and B^3 are significant. For a factor to affect the change, the value in Table 3 in the last column should be lower than 0.05. The model F-value of 2556.94 implies the model is significant, and the lack of fit F-value of 5.54 implies there is a 9.84% chance that a lack of fit F-value this large could occur due to noise. Although this is still a relatively low value, a non-significant lack of fit means that the parameters are well chosen and there are no major errors in the choice of factors and model.

Table 2. Results for the upper level of the working chamber.

Run	Factor A: Hatch Distance *HD*, mm	Factor B: Orientation α, °	Tensile Strength σ_m, MPa	Length *l*, mm	Thickness *h*, mm	Width *b*, mm
1	0.23	0	~~46.27 ± 0.138~~	~~149.81 ± 0.05~~	~~4.15 ± 0.03~~	~~10.01 ± 0.03~~
2	0.6	0	~~8.16 ± 0.870~~	150.19 ± 0.02	4.39 ± 0.09	9.89 ± 0.04
3	0.23	60	~~43.62 ± 0.760~~	~~150.11 ± 0.06~~	~~4.07 ± 0.03~~	~~10.10 ± 0.01~~
4	0.6	60	10.79 ± 0.914	150.35 ± 0.07	4.09 ± 0.01	10.20 ± 0.02
5	0.23	30	~~44.09 ± 0.836~~	149.83 ± 0.04	4.12 ± 0.02	10.03 ± 0.04
6	0.6	30	~~10.03 ± 1.104~~	~~150.14 ± 0.02~~	~~4.30 ± 0.03~~	~~9.87 ± 0.01~~
7	0.42	0	30.62 ± 1.428	150.10 ± 0	4.04 ± 0.02	9.91 ± 0.02
8	0.42	60	29.07 ± 1.127	150.38 ± 0.05	4.03 ± 0.04	10.09 ± 0.04
9	0.32	15	42.41 ± 0.662	149.93 ± 0.03	4.12 ± 0	10.03 ± 0.03
10	0.51	15	16.93 ± 0.608	150.13 ± 0.07	4.19 ± 0.05	9.96 ± 0.04
11	0.32	45	39.75 ± 0.621	150.09 ± 0.04	4.09 ± 0.02	10.03 ± 0.03
12	0.51	45	17.86 ± 1.032	150.33 ± 0.03	4.11 ± 0.04	9.98 ± 0.09
13	0.32	30	41.66 ± 0.784	149.99 ± 0.02	4.10 ± 0.02	9.98 ± 0.02
14	0.51	30	17.62 ± 1.093	150.23 ± 0.02	4.11 ± 0.01	10.01 ± 0.05
15	0.42	15	31.77 ± 1.088	150.13 ± 0.04	4.11 ± 0.01	9.98 ± 0.06
16	0.42	45	29.21 ± 1.146	150.29 ± 0.03	4.07 ± 0.02	10.01 ± 0.03
17	0.42	30	31.28 ± 1.636	150.14 ± 0.04	4.10 ± 0.02	9.95 ± 0.04
18	0.42	30	31.30 ± 0.167	150.09 ± 0.05	4.12 ± 0.06	9.94 ± 0.05
19	0.42	30	31.00 ± 1.341	150.10 ± 0.09	4.00 ± 0	9.96 ± 0.02
20	0.42	30	31.20 ± 0.356	150.12 ± 0.09	4.09 ± 0.03	9.93 ± 0.04

Experiment runs 1, 3, and 6 were discarded from further analysis, and additionally, runs 2 and 5 for tensile strength since the analysis has shown that the response at those points does not correspond to the model, i.e., the deviations in dimensions and tensile strength values from other data are significant (strikethrough text).

Table 3. Analysis according to ANOVA for the tensile strength for the upper level of the working chamber.

	Sum of Squares	Degrees of Freedom DF	Mean Square	F Value	*p*-Value (Risk of Rejection of H_0)
Model	1215.54	9	135.06	2556.94	<0.0001 significant
A	40.02	1	70.02	1325.54	<0.0001
B	2.76	1	2.76	52.19	0.0008
AB	3.22	1	3.22	61.00	0.0006
A^2	7.38	1	7.38	139.68	<0.0001
B^2	2.54	1	2.54	48.01	0.0010
A^2B	0.9577	1	0.9577	18.13	0.0080
AB^2	0.0420	1	0.0420	0.7953	0.4134
A^3	0.0	1	0.0	0.0009	0.9773
B^3	1.27	1	1.27	24.13	0.0044
Residual	0.2647	5	0.0528		
Lack of fit	0.2078	2	0.1039	5.54	0.0984 not significant
Pure error	0.0563	3	0.0188		
Cor Total	1215.81	14			

Table 4 shows statistics for tensile strength in the upper part of the working chamber. Apart from the fact that R^2 is a sign that the model follows the data very well (the closer it is to 1, the better the model is), at the same time, adeq precision measures the signal-to-noise ratio, and it is important that the difference is greater than 4. In this analysis, the ratio of 168.6247 indicates an adequate signal, and this model can be used to navigate the model design.

Table 4. Fit statistics for the tensile strength at the upper level of the working chamber.

	Tensile Strength σ_m, N/mm^2
Standard deviation	0.2298
Mean	28.83
Coefficient of determination (*R*-squared (R^2))	0.9998
Adjusted R^2	0.9994
Adeq Precision	168.6247

Tensile strength can be described by an equation with actual parameters:

$$\sigma_m = 23.9 + 175.7 \times HD + 1.3 \times \alpha - 5.3 \times HD \times \alpha - 391.2 \times HD^2 - 0.013 \times \alpha^2 + 6.6 \times HD^2 \times \alpha + 0.0085 \times HD \times \alpha^2 + 13.9 \times HD^3 + 0.00009 \times \alpha^3 \quad (4)$$

where σ_m [N/mm^2]—tensile strength, *HD* [mm]—hatch distance, and α [°]—orientation.

Figure 5 shows the dependence of tensile strength on the hatch distance and orientation. The lowest value of tensile strength is 10.79 N/mm^2, which happened at the largest hatch distance and the smallest orientation, while the highest measured value is 42.41 N/mm^2 for the hatch distance of 0.32 mm and the orientation of 15°. However, the values for the tensile strength can be read from the diagram for any combination of input parameters within selected limits.

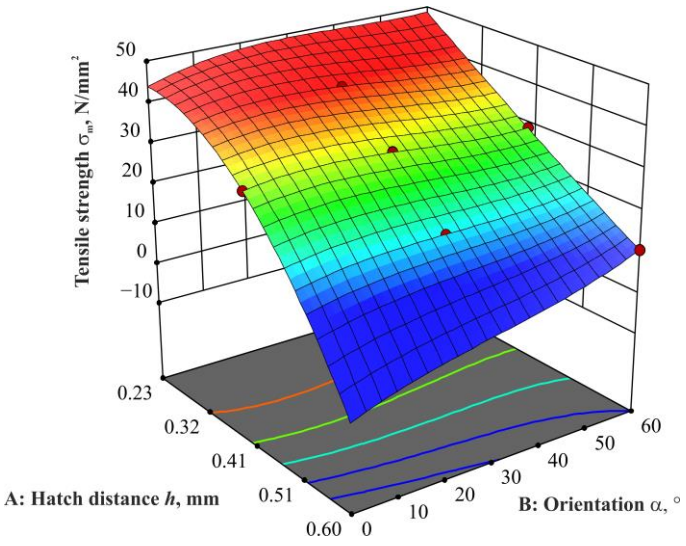

Figure 5. Dependence of hatch distance and orientation on the tensile strength in the upper part of the working chamber.

3.1.2. Results for Length in the Upper Level of the Working Chamber

A quadratic model was chosen for the length results in the upper level of the chamber, and from Table 5, it can be seen that the influencing factors are A, B, A^2, and B^2.

Table 6 shows statistics for length in the upper part of the working chamber. The difference between the predicted R^2 of 0.7657 and the adjusted R^2 of 0.9327 is less than 0.2. Furthermore, the adeq precision ratio of 25.7796 indicates an adequate signal, which indicates a well-chosen model.

Table 5. Analysis according to ANOVA for the length of the upper level of the working chamber.

	Sum of Squares	Degrees of Freedom DF	Mean Square	F Value	*p*-Value (Risk of Rejection of H_0)
Model	0.3265	5	0.0653	45.35	<0.0001 significant
A	0.1215	1	0.1215	84.40	<0.0001
B	0.0809	1	0.0809	56.22	<0.0001
AB	0.0047	1	0.0047	3.26	0.0984
A^2	0.0399	1	0.0399	27.73	0.0003
B^2	0.0179	1	0.0179	12.42	0.0048
Residual	0.0158	11	0.0014		
Lack of fit	0.0144	8	0.0018	3.65	0.1573 not significant
Pure error	0.0015	3	0.0005		
Cor Total	0.3423	16			

Table 6. Fit statistics for the length of the upper level of the working chamber.

	Length *l*, mm
Standard deviation	0.0379
Mean	150.14
Coefficient of determination (*R*-squared (R^2))	0.9537
Adjusted R^2	0.9327
Predicted R^2	0.7657
Adeq Precision	25.7796

Length can be described by an equation with actual parameters:

$$l = 148.8 + 4.8 \times HD + 0.002 \times \alpha - 0.01 \times HD \times \alpha - 4.2 \times HD^2 + 0.00011 \times \alpha^2 \quad (5)$$

where l [mm]—length, HD [mm]—hatch distance, and α [°]—orientation.

According to the contours below the diagram (Figure 6), the values of the factors that achieve lengths of 150 mm are clearly visible. In the case of dimensions, the aim is to achieve 150 × 4 × 10 mm, which are the dimensions of the test specimens according to the ISO 527 standard [18].

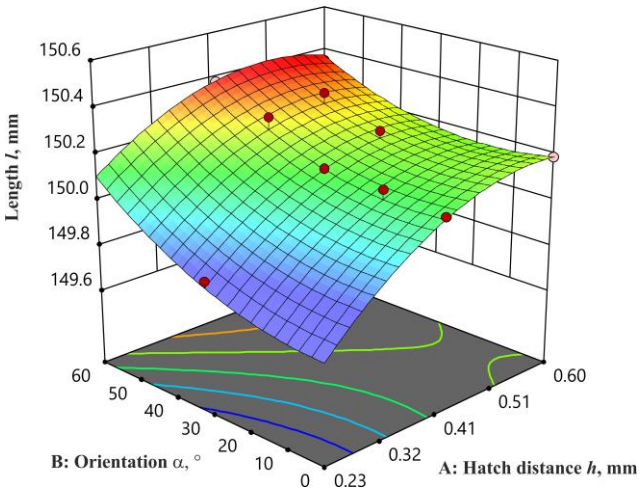

Figure 6. Dependence of hatch distance and orientation on the length of the upper part of the working chamber. The red and pink points on the diagram represent the design points below and above the surface.

3.1.3. Results for Thickness in the Upper Level of the Working Chamber

A quadratic model was chosen for thickness analysis, but factor B^2 has a *p*-value of 0.3034, which shows that it has no influence on thickness, and at the same time, predicted R^2 is not close to adjusted R^2, as would normally be expected (the difference is more than 0.2, which may indicate a large block effect or a possible problem with the model or data), and it is necessary to reduce the model. Accordingly, factor B^2 was excluded from the analysis, and after that, the data were processed and presented in Tables 7 and 8. From Table 7, it can be seen that the influencing factors on the thickness in the upper level of the chamber are A, AB, and A^2, and there is an 87.69% chance that lack of fit can occur due to noise, which indicates that the error is not significant. A non-significant lack of fit is good; we want the model to fit.

Table 7. Analysis according to ANOVA for the thickness at the upper level of the working chamber.

	Sum of Squares	**Degrees of Freedom DF**	**Mean Square**	**F Value**	***p*-Value (Risk of Rejection of H_0)**
Model	0.0930	4	0.0232	15.04	0.0001 significant
A	0.0100	1	0.0100	6.44	0.0260
B	0.0031	1	0.0031	2.00	0.1828
AB	0.0195	1	0.0195	12.65	0.0039
A^2	0.0263	1	0.0263	17.01	0.0014
Residual	0.0185	12	0.0015		
Lack of fit	0.0101	9	0.0011	0.3958	0.8769 not significant
Pure error	0.0085	3	0.0028		
Cor Total	0.1115	16			

Table 8. Fit statistics for the thickness at the upper level of the working chamber.

	Thickness *h*, mm
Standard deviation	0.0393
Mean	4.11
Coefficient of determination (*R*-squared (R^2))	0.8337
Adjusted R^2	0.7783
Predicted R^2	0.6109
Adeq Precision	15.5986

Table 8 shows statistics for thickness in the upper part of the working chamber. The predicted R^2 of 0.6109 is in reasonable agreement with the adjusted R^2 of 0.7783, i.e., the difference is less than 0.2.

Thickness can be described by an equation with actual parameters:

$$h = 4.31 - 1.86 \times HD + 0.0075 \times \alpha - 0.0204 \times HD \times \alpha + 3.29 \times HD^2 \quad (6)$$

where *h* [mm]—thickness, *HD* [mm]—hatch distance, and α [°]—orientation.

From the diagram in Figure 7, values of 4 mm are achieved for any value of orientation, but in the value of hatch distance, from 0.23 to 0.41 mm.

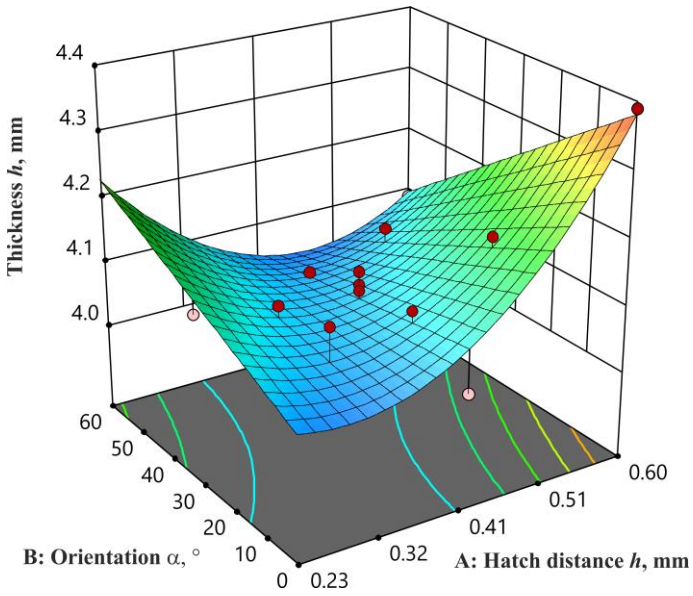

Figure 7. Dependence of hatch distance and orientation on the thickness in the upper part of the working chamber.

3.1.4. Results for Width in the Upper Level of the Working Chamber

A modified cubic model was chosen for the width analysis. Although according to the results shown in Table 9, it can be noticed that the input factors A and B alone do not affect the width, all other combinations do, namely: AB, A^2, B^2, AB^2, A^3, and B^3. The modified model was chosen because the A^2B combination was also excluded from the analysis because such a combination has no influence, but when it is excluded from the analysis, then the AB factor combination also becomes influential on the width. The model F-value of 22.36 implies the model is significant and a lack of fit F-value of 3.80 implies the lack of fit is not significant relative to the pure error.

Table 9. Analysis according to ANOVA for the width at the upper level of the working chamber.

	Sum of Squares	Degrees of Freedom DF	Mean Square	F Value	*p*-Value (Risk of Rejection of H_0)
Model	0.0821	8	0.0103	22.36	<0.0001 significant
A	0.0004	1	0.0004	0.8086	0.3948
B	0.0001	1	0.0001	0.1519	0.7069
AB	0.0039	1	0.0039	8.54	0.0192
A^2	0.0073	1	0.0073	15.92	0.0040
B^2	0.0041	1	0.0041	8.97	0.0172
AB^2	0.0035	1	0.0035	7.66	0.0244
A^3	0.0027	1	0.0027	5.99	0.0401
B^3	0.0054	1	0.0054	11.83	0.0088
Residual	0.0037	8	0.0005		
Lack of fit	0.0032	5	0.0006	3.80	0.1503 not significant
Pure error	0.0005	3	0.0002		
Cor Total	0.0858	16			

Table 10 shows statistics for width in the upper part of the working chamber. The ratio of 19.314 indicates an adequate signal, which means that this model can be used for analysis.

Table 10. Fit statistics for the width of the upper level of the working chamber.

	Width *b*, mm
Standard deviation	0.0214
Mean	9.99
Coefficient of determination (*R*-squared (R^2))	0.9572
Adjusted R^2	0.9144
Predicted R^2	0.1255
Adeq Precision	19.314

Width can be described by an equation with actual parameters:

$$b = 10.14 + 3.54 \times HD - 0.03 \times \alpha + 0.088 \times HD \times \alpha - 17.15 \times HD^2 + 0.0003 \times \alpha^2 - 0.0013 \times HD \times \alpha^2 + 17.63 \times HD^3 + 3.84 \times 10^{-6} \times \alpha^3 \quad (7)$$

where b [mm]—width, HD [mm]—hatch distance, and α [°]—orientation.

To achieve a width of 10 mm, it is necessary to select processing parameters according to the turquoise curve shown as a contour (lower surface) in the diagram itself (Figure 8).

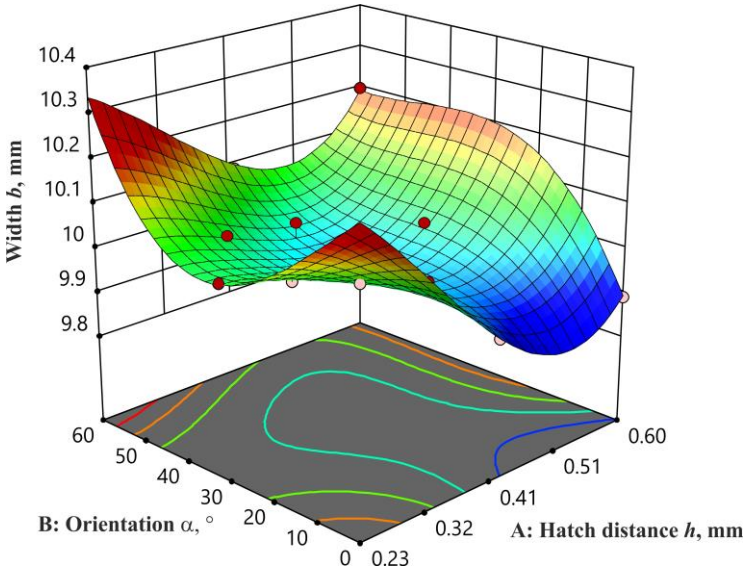

Figure 8. Dependence of hatch distance and orientation on the width in the upper part of the working chamber.

3.2. Results for Dimensions and Tensile Strength for the Lower Level of the Working Chamber

Table 11 shows the arithmetic means and standard deviations of the tensile strength and dimensions (length, width, and thickness) of lower level of the working chamber.

3.2.1. Results for Tensile Strength in the Lower Level of the Working Chamber

The model F-value of 1704.10 implies the model is significant. There is only a 0.01% chance that an F-value this large could occur due to noise. *p*-values less than 0.0500 indicate model terms are significant. In this case, A, B, AB, A^2, A^2B, and A^3 are significant model terms. If there are many insignificant model terms (not counting those required to support hierarchy), model reduction must be carried out. The lack of fit F-value of 25.46 implies that the lack of fit is significant. There is only a 1.10% chance that a lack of fit F-value this large could occur due to noise. A significant lack of fit is not good because we want the model to fit.

Table 11. Results for the lower level of the working chamber.

Run	Factor A: Hatch Distance *HD*, mm	Factor B: Orientation α, °	Tensile Strength σ_m, MPa	Length *l*, mm	Thickness *h*, mm	Width *b*, mm
1	0.23	0	47.21 ± 0.935	149.77 ± 0.05	4.21 ± 0.03	10.0 ± 0.03
2	0.6	0	8.41 ± 0.946	150.13 ± 0.01	4.44 ± 0.06	9.89 ± 0.02
3	0.23	60	44.55 ± 1.128	150.0 ± 0	4.07 ± 0.04	10.03 ± 0.01
4	0.6	60	10.79 ± 0.530	150.35 ± 0.10	4.08 ± 0.05	10.17 ± 0.08
5	0.23	30	44.9 ± 0.805	149.79 ± 0.01	4.11 ± 0.05	9.99 ± 0.02
6	0.6	30	10.21 ± 1.073	150.12 ± 0.05	4.19 ± 0.08	9.97 ± 0.04
7	0.42	0	33.21 ± 1.448	150.0 ± 0	4.07 ± 0.02	9.87 ± 0.01
8	0.42	60	29.22 ± 0.603	150.43 ± 0.10	4.03 ± 0.03	10.08 ± 0.02
9	0.32	15	43.3 ± 1.320	149.96 ± 0.04	4.10 ± 0.03	9.98 ± 0.02
10	0.51	15	17.72 ± 0.244	150.19 ± 0.01	4.14 ± 0.03	9.97 ± 0.03
11	0.32	45	41.09 ± 0.811	150.07 ± 0.06	4.08 ± 0.02	9.97 ± 0.02
12	0.51	45	17.82 ± 0.621	150.30 ± 0.03	4.08 ± 0.05	9.99 ± 0.01
13	0.32	30	42.29 ± 0.839	149.98 ± 0.02	4.09 ± 0.01	9.95 ± 0.06
14	0.51	30	17.62 ± 0.335	150.18 ± 0.02	4.11 ± 0.01	10.01 ± 0.06
15	0.42	15	31.82 ± 0.734	150.09 ± 0.01	4.11 ± 0.03	9.95 ± 0.06
16	0.42	45	29.72 ± 0.992	150.24 ± 0.02	4.07 ± 0.01	9.95 ± 0.05
17	0.42	30	31.87 ± 1.218	150.14 ± 0.13	4.06 ± 0.02	9.93 ± 0.03
18	0.42	30	31.82 ± 0.502	150.10 ± 0.1	4.01 ± 0.01	9.96 ± 0.04
19	0.42	30	31.72 ± 1.073	150.14 ± 0.06	4.02 ± 0.01	9.95 ± 0.06
20	0.42	30	31.60 ± 1.496	150.08 ± 0.03	4.03 ± 0.01	9.92 ± 0.04

According to the analysis (Tables 12 and 13), it can be concluded that the chosen model, regardless of the excellent R^2 value of 0.9987 and many influencing factors, cannot be chosen to describe the tensile strength at the lower level of the chamber. Otherwise, exclusion of certain test conditions and exclusion of non-influential factors can lead to a reduction of the model error or to an increase of the model to the fifth, sixth, and higher levels; in this case, it did not help either, as it was the case for the tensile strength in the upper level of the chamber. For the tensile strength at the lower level of the chamber, it is necessary to carry out additional analyses or include additional processing parameters with orientation and hatch distance.

Table 12. Analysis according to ANOVA for the tensile strength at the lower level of the working chamber.

	Sum of Squares	Degrees of Freedom DF	Mean Square	F Value	*p*-Value (Risk of Rejection of H_0)
Model	2882.51	6	480.42	1704.10	<0.0001 significant
A	593.01	1	593.01	2103.48	<0.0001
B	11.04	1	11.04	39.16	<0.0001
AB	7.43	1	7.43	26.34	0.0002
A^2	46.02	1	46.02	163.23	<0.0001
A^2B	5.69	1	5.69	20.19	0.0006
A^3	52.77	1	52.77	187.20	<0.0001
Residual	3.66	13	0.2819		
Lack of fit	3.62	10	0.3622	25.46	0.0110 significant
Pure error	0.0427	3	0.0142		
Cor Total	2886.18	19			

Table 13. Fit statistics for the tensile strength at the lower level of the working chamber.

	Tensile Strength σ_m, N/mm^2
Standard deviation	0.5310
Mean	29.84
Coefficient of determination (*R*-squared (R^2))	0.9987
Adjusted R^2	0.9981
Predicted R^2	0.9946
Adeq Precision	122.2254

3.2.2. Results for Length in the Lower Level of the Working Chamber

The cubic model was chosen for the analysis because it best describes the length at the lower level of the chamber. According to Table 14, the influencing factors on the length are A, B, A^2, B^2, A^2B, and B^3. There is an 86.68% lack of fit, which indicates a non-significant error in the chosen model. Furthermore, the statistical parameters (Table 15) indicate that the model is well chosen.

Table 14. Analysis according to ANOVA for the length at the lower level of the working chamber.

	Sum of Squares	**Degrees of Freedom DF**	**Mean Square**	**F Value**	***p*-Value (Risk of Rejection of H_0)**
Model	0.5049	9	0.0561	90.51	<0.0001 significant
A	0.0461	1	0.0461	74.38	<0.0001
B	0.0111	1	0.0111	17.90	0.0017
AB	0.0000	1	0.0000	0.0380	0.8494
A^2	0.0815	1	0.0815	131.57	<0.0001
B^2	0.0294	1	0.0294	47.50	<0.0001
A^2B	0.0145	1	0.0145	23.35	0.0007
AB^2	0.0003	1	0.0003	0.4377	0.5232
A^3	0.0028	1	0.0028	4.58	0.0581
B^3	0.0055	1	0.0055	8.92	0.0136
Residual	0.0062	10	0.0006		
Lack of fit	0.0029	7	0.0004	0.3825	0.8668 not significant
Pure error	0.0033	3	0.0011		
Cor Total	0.5111	19			

Table 15. Fit statistics for the length at the lower level of the working chamber.

	Length *l*, mm
Standard deviation	0.0249
Mean	150.10
Coefficient of determination (*R*-squared (R^2))	0.9879
Adjusted R^2	0.9770
Predicted R^2	0.9607
Adeq Precision	38.2619

Length can be described by an equation with actual parameters:

$$l = 149.9 - 2.98 \times HD - 0.008 \times \alpha + 0.078 \times HD \times \alpha + 12.28 \times HD^2 - 0.00026 \times \alpha^2 - 0.1007 \times HD^2 \times \alpha + 0.00009 \times HD \times \alpha^2 - 11.3 \times HD^3 + 3.7 \times 10^{-6} \times \alpha^3 \quad (8)$$

where l [mm]—length, HD [mm]—hatch distance, and α [°]—orientation.

In Figure 9, the turquoise line represents the length dimension of 150 mm. When following this line, it can be concluded that 150 mm is achieved by changing the orientation in the entire observed area, but within the limits of hatch distance from 0.23 to a maximum of 0.41 mm.

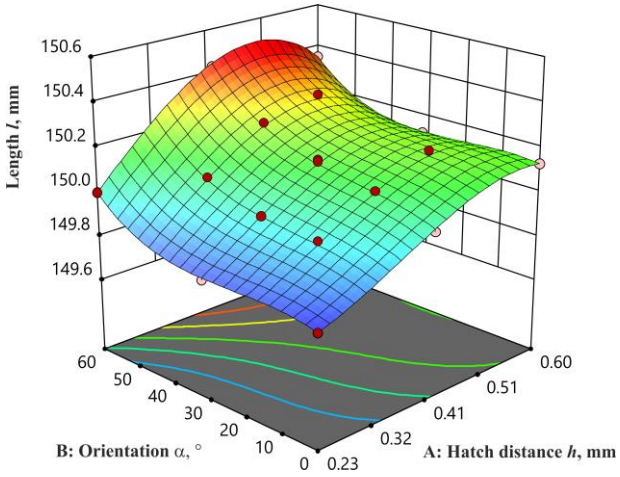

Figure 9. Dependence of hatch distance and orientation on the length in the lower part of the working chamber.

3.2.3. Results for Thickness in the Lower Level of the Working Chamber

A modified quadratic model was chosen for data analysis for the thickness at the lower level of the working chamber. The combination of factors A^2B was added to the analysis because, in addition to A, AB, and A^2, they have a great influence on the thickness (Table 16). The factor B itself, including B^2, has no influence on the thickness at the lower level of the chamber, which is correlated with the thickness at the upper level of the chamber.

Table 16. Analysis according to ANOVA for the thickness at the lower level of the working chamber.

	Sum of Squares	Degrees of Freedom DF	Mean Square	F Value	*p*-Value (Risk of Rejection of H_0)
Model	0.1560	6	0.0260	30.39	<0.0001 significant
A	0.0163	1	0.0163	19.09	0.0008
B	0.0014	1	0.0014	1.69	0.2161
AB	0.0124	1	0.0124	14.55	0.0021
A^2	0.0431	1	0.0431	50.40	<0.0001
B^2	0.0017	1	0.0017	1.97	0.1840
A^2B	0.0175	1	0.0175	20.42	0.0006
Residual	0.0111	13	0.0009		
Lack of fit	0.0097	10	0.0010	2.08	0.2967 not significant
Pure error	0.0014	3	0.0005		
Cor Total	0.1671	19			

Table 17 shows statistics for thickness at the lower part of the working chamber. The ratio of 21.6297 indicates an adequate signal, which means that this model can be used to navigate the design space.

Table 17. Fit statistics for the thickness at the lower level of the working chamber.

	Thickness *h*, mm
Standard deviation	0.0292
Mean	4.10
Coefficient of determination (*R*-squared (R^2))	0.9335
Adjusted R^2	0.9027
Predicted R^2	0.7128
Adeq Precision	21.6297

Thickness can be described by an equation with actual parameters:

$$h = 4.99 - 4.86 \times HD - 0.016 \times \alpha + 0.073 \times HD \times \alpha + 6.52 \times HD^2 + 0.000026 \times \alpha^2 - 0.10009 \times HD^2 \times \alpha \quad (9)$$

where h [mm]—thickness, HD [mm]—hatch distance, and α [°]—orientation.

For an approximate hatch distance of 0.37 mm, a thickness value of the nearest 4 mm can be obtained for all orientations, which can be seen in the diagram (Figure 10), that is, the area between the two turquoise lines. In this case, a value of exactly 4 mm cannot be achieved with any combination of parameters.

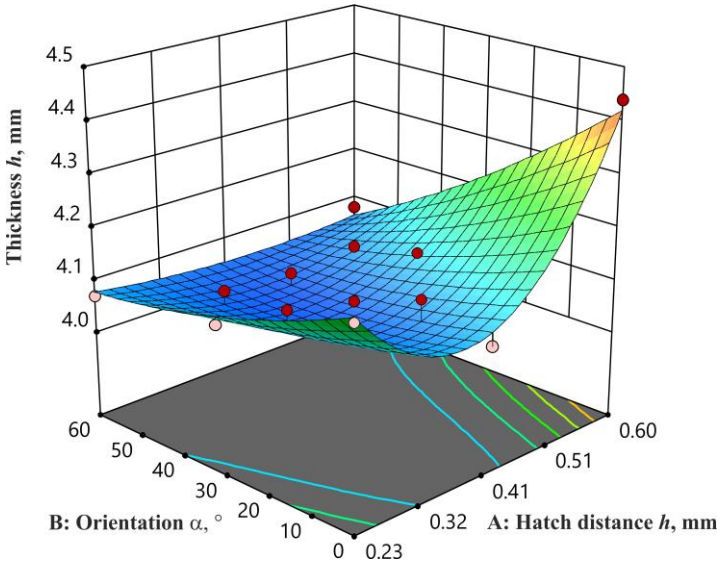

Figure 10. Dependence of hatch distance and orientation on the thickness in the lower part of the working chamber.

3.2.4. Results for Width at the Lower Level of the Working Chamber

According to Table 18, it can be noted that a modified cubic model was chosen for the analysis of the width value in the lower level of the working chamber. The values that are deleted from the cubic model have no influence on the width, and with them, an inadequate model is achieved, and they must be removed from the analysis. In the case of the width for the lower level of the chamber, factors AB, A^2, B^2, and B^3 have an influence. Individually, factors A and B have no effect on the width.

Table 18. Analysis according to ANOVA for the width at the lower level of the working chamber.

	Sum of Squares	Degrees of Freedom DF	Mean Square	F Value	*p*-Value (Risk of Rejection of H_0)
Model	0.0742	6	0.0124	25.89	<0.0001 significant
A	0.0003	1	0.0003	0.5650	0.4656
B	0.0005	1	0.0005	1.04	0.3267
AB	0.0156	1	0.0156	32.65	<0.0001
A^2	0.0053	1	0.0053	11.08	0.0054
B^2	0.0028	1	0.0028	5.76	0.0321
B^3	0.0083	1	0.0083	17.44	0.0011
Residual	0.0062	13	0.0005		
Lack of fit	0.0052	10	0.0005	1.56	0.3933 not significant
Pure error	0.0010	3	0.0003		
Cor Total	0.0805	19			

Table 19 shows the results of the statistics for width in the lower part of the working chamber. The predicted R^2 of 0.7984 follows the date for the adjusted R^2 of 0.8871. In this model, a ratio of 22.772 for adeq precision indicates an adequate signal.

Table 19. Fit statistics for the width at the lower level of the working chamber.

	Width *b*, mm
Standard deviation	0.0219
Mean	9.98
Coefficient of determination (*R*-squared (R^2))	0.9228
Adjusted R^2	0.8871
Predicted R^2	0.7984
Adeq Precision	22.772

Width can be described by an equation with actual parameters:

$$b = 10.23 - 1.32 \times HD + 0.004 \times \alpha + 0.0109 \times HD \times \alpha + 1.23 \times HD^2 - 0.00034 \times \alpha^2 + 4.12 \times 10^{-6} \times \alpha^3 \quad (10)$$

where b [mm]—width, HD [mm]—hatch distance, and α [°]—orientation.

Obtaining a value of 10 mm for the width in the lower part of the working chamber is possible for the orientation from 30° to 50° in the entire range of hatch distance limits, which can be observed in Figure 11.

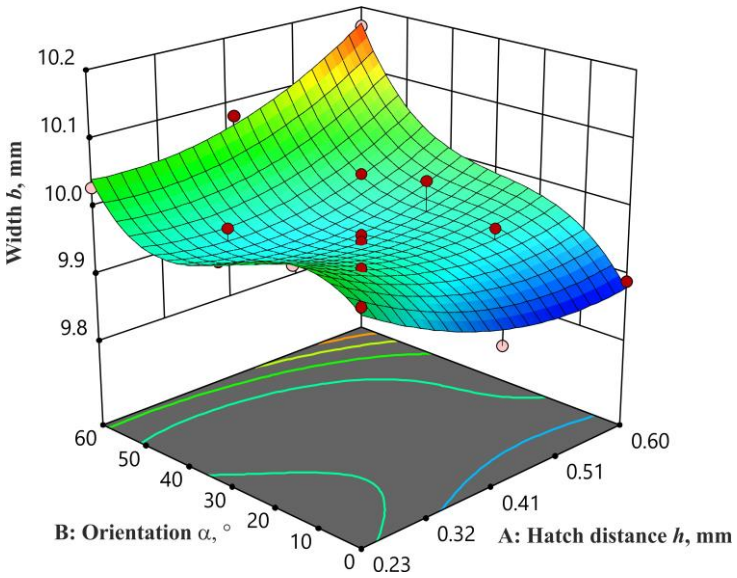

Figure 11. Dependence of hatch distance and orientation on the width in the lower part of the working chamber.

3.3. Optimization

For performing desirability optimization, input parameters can be optimized. The optimization process searches for a combination of factor values that simultaneously satisfy the criteria (wishes and priorities) placed on each of the responses and factors. Optimization can be displayed numerically and graphically. Numerical optimization uses the models to search the factor space for the best trade-offs to achieve multiple goals. For numerical optimization, the possible goals can be set to maximize, minimize, target, within range, none (for responses only), and set to an exact value (factors only). The goals are combined into an overall desirability function. Graphical optimization uses the models to show the volume where acceptable response outcomes can be found.

In this research, the optimization criteria (for an optimal solution) were maximum tensile strength and target values for dimension (length × thickness × width of 150 × 4 × 10 mm) with input factors orientations and hatch distance within the chosen limits of the experiment. The combination of the selected values for optimization of products produced with selected parameters gives results presented in Table 20 for the upper part

of the working chamber and in Table 21 for the lower part of the working chamber. The upper and lower limits of the dimensions in the optimization were chosen in accordance with the permitted tolerance specified in the ISO 527 standard [18] for the production of test specimens for testing tensile properties.

Table 20. Criteria and solution for the upper part of the working chamber.

Name	Goal	Lower Limit	Upper Limit	Solution
Factor A: hatch distance, mm	is in range	0.23	0.6	0.295
Factor B: orientation, °	is in range	0	60	45.6
Tensile strength, N/mm^2	max	8.16	46.27	42.53
Length, mm	is target = 150	148	152	150.07
Thickness, mm	is target = 4	3.8	4.2	4.08
Width, mm	is target = 10	9.8	10.2	10.0

Table 21. Criteria and solution for the lower part of the working chamber.

Name	Goal	Lower Limit	Upper Limit	Solution
Factor A: hatch distance, mm	is in range	0.23	0.6	0.266
Factor B: orientation, °	is in range	0	60	55.5
Tensile strength, N/mm^2	max	8.41	47.21	44.5
Length, mm	is target = 150	148	152	150.04
Thickness, mm	is target = 4	3.8	4.2	4.07
Width, mm	is target = 10	9.8	10.2	10.0

For the upper level of the working chamber, two solutions were found with a desirability of d = 0.843 (Table 20).

The desirability curve for the upper part of the working chamber within the optimization constraints is shown in Figure 12.

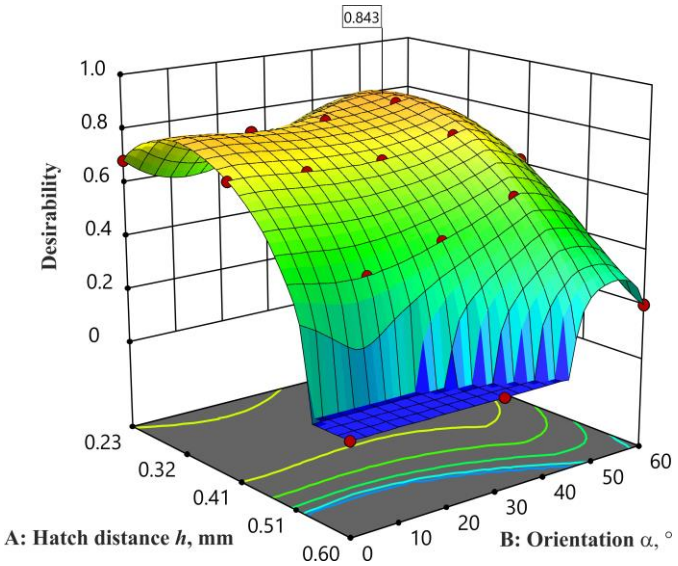

Figure 12. Desirability curve for the solution of the upper part of the working chamber according to Table 20.

For the lower level of the working chamber, two solutions were found with a desirability of d = 0.877 (Table 21).

The desirability curve for the lower part of the working chamber within the optimization constraints is shown in Figure 13.

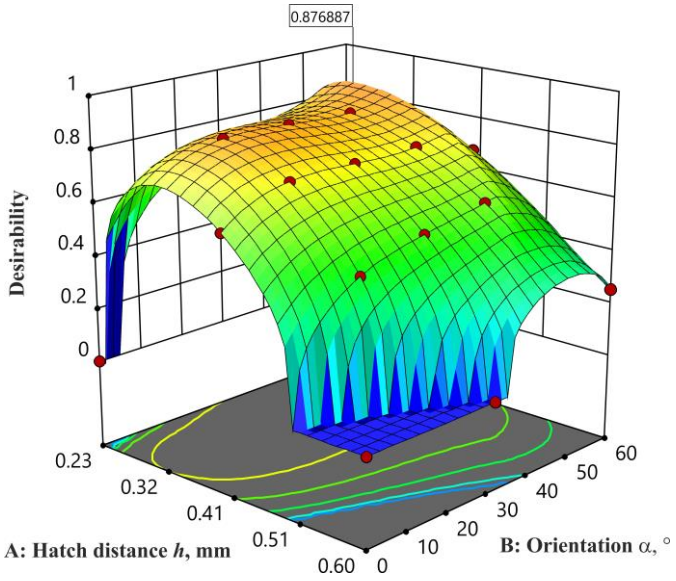

Figure 13. Desirability curve for the solution of the lower part of the working chamber according to Table 21.

4. Discussion

When comparing the tensile strength results from El Magri et al. [14] with the obtained mean strength results in this test, the values are equal. However, when choosing the parameters with a hatch distance of 0.295 mm and orientation of 45° in the upper level and a hatch distance of 0.266 mm and orientation of 55° in the lower level, tensile strength values of 43 N/mm^2 are achieved, which is a 37% higher value.

Working with different orientations, Stoia et al. [13] managed to obtain a maximum tensile strength of 33 N/mm^2, which correlates with the mean value in both levels in this experiment, certainly less than the maximum value of 47 N/mm^2.

Matuš et al. determined that altering only the orientation of the product (along the *x*-*y*-*z* axis) within the working chamber resulted in measured values displaying predominantly positive deviations in length along the *x* axis. Conversely, deviations measured along the *y* axis were predominantly negative. The smallest length deviations occurred when the product was rotated successively by 90°, 90°, and 0°, followed by 0°, 90°, and 90°, and, finally, 90°, 90°, and 90° along the *x*, *y*, and *z* axes, respectively [20]. To compare these results with those obtained in this experiment, it can be concluded that the orientation in the *z* axis must be 45° for the upper level in the working chamber and 55° for the lower level to achieve minimal dimensional deviations, which the authors in paper [20] established for the orientation in the *z* axis exclusively 0° and/or 90°. However, the achievement of minimal dimensional deviations also depends on the other processing parameters, which Matuš et al. did not include in their experiment.

Korycki et al. analyzed the influence of laser power, hatch distance, and energy density on mechanical properties and concluded that with a hatch distance of 0.16 mm, a tensile strength of 42 N/mm^2 is achieved [21]. Upon comparison with the proposed test, this value is achieved at a hatch distance of 0.29 mm, regardless of whether it is situated at the upper or lower level of the chamber.

The study by Gazzerro et al. [22] merits attention as it aligns with a comparable approach to this work. However, in Gazzerro et al.'s study, they evaluated flexural and shear properties using original and recycled materials across two levels, with the upper level positioned at a height of 50 mm. The results of the tests conducted showed that the products with the best flexural properties are those made in the central zone of the working chamber, and the dimensions show that there is no difference between those built on the upper and lower parts of the working chamber, which is comparable to the analyses conducted in this experiment. Gazzerro et al. also stated that only thickness shows the

lowest deviations along the z axis. This stands in contrast to the tests conducted in this paper, as the analysis revealed no difference in dimensional stability between the initial level of 6 mm and the subsequent level of 174 mm. However, in the mentioned work, the authors utilized only one orientation of the test specimens along the x-y axes (0°).

The influence of orientation on the mechanical properties of PA12 in the SLS process was published in the paper [23] authored by Ruivo et al. Through the comparison of four different orientations, they concluded that the best mechanical properties are exhibited by the edge 0° orientation in the horizontal plane XX axis. These tests are in total contrast to the tests of Jevtić et al., where they compared horizontal and vertical printing orientations on tensile strength and determined that test specimens in horizontal orientations exhibit the lowest tensile strength and larger deformations in comparison with test specimens in vertical orientation [24]. In our tests, the z-axis orientation of 45° in the upper level and the orientation of 55° in the lower part of the working chamber gave optimal tensile strength and dimensional stability (Tables 20 and 21).

5. Conclusions

In selective laser sintering, apart from power and speed, the hatch distance significantly impacts the properties (mechanical properties or dimensional stability), as described in the Section 1. While the premise of these tests suggested that modifying the input parameters at distinct levels within the working chamber would result in varying properties, this assumption remained unverified. The results showed that when looking at dimensional stability, the same parameters affect the length, thickness, and width, regardless of whether the product is manufactured in the lower half or upper half of the chamber along the z-axis. Consequently, the length was affected by both input factors, the thickness primarily by factor A and certain combinations, whereas in the case of the width, factors A (hatch distance) and B (orientation) individually held no influence, but only their combined effects mattered. Therefore, the initial hypothesis regarding dimensional stability was rejected. After optimization, for the desired dimensions of the test specimen (150 × 4 × 10 mm), the optimal processing parameters were determined. For the upper level, hatch distance should be 0.295 mm and orientation 45.6°, while for the lower level, hatch distance should be 0.266 mm and orientation 55.5°. In the case of the tensile strength, it was not possible to carry out the analysis at the lower level, and the conclusion is that it is easier to obtain good tensile strength at the upper level with selected processing parameters (hatch distance and orientation). An average value of only 30 N/mm^2 is obtained, which is quite low for polyamide obtained by selective laser sintering.

Author Contributions: Conceptualization, A.P. and P.I.; methodology, A.P.; validation, A.P.; formal analysis, A.P., P.I., M.T. and M.R.H.; investigation, A.P.; data curation, A.P. and M.R.H.; writing—original draft preparation, A.P.; writing—review and editing, P.I. and M.R.H.; visualization, A.P., M.T. and P.I. All authors have read and agreed to the published version of the manuscript.

Funding: This research received no external funding.

Institutional Review Board Statement: Not applicable.

Informed Consent Statement: Not applicable.

Data Availability Statement: The raw data supporting the conclusions of this article will be made available by the authors on request.

Acknowledgments: The authors would like to thank the company Klex d.o.o. for the production of test specimens with the process of selective laser sintering.

Conflicts of Interest: The authors declare no conflicts of interest.

References

1. Pilipović, A.; Valentan, B.; Brajlih, T.; Haramina, T.; Balič, J.; Kodvanj, J.; Šercer, M.; Drstvenšek, I. Influence of laser sintering parameters on mechanical properties of polymer products. In Proceedings of the 3nd International Conference on Additive Technologies: iCAT 2010 DAAAM International, Nova Gorica, Slovenia, 22–24 September 2010.
2. Godec, D.; Šercer, M.; Rujnić-Sokele, M. Influence of hybrid mould on moulded parts properties. *Rapid Prototyp. J.* **2008**, *14*, 95–101. [CrossRef]
3. Drstvenšek, I.; Ihan Hren, N.; Strojnik, T.; Brajlih, T.; Valentan, B.; Pogačar, V.; Županšić Hartner, T. Applications of Rapid Prototyping in Cranio-Maxilofacial Surgery Procedures. *Int. J. Biol. Biomed. Eng.* **2008**, *2*, 29–38.
4. İlkgün, Ö. Effects of Production Parameters on Porosity and Hole Properties in Laser Sintering Rapid Prototyping Process. Master's Thesis, The Graduate School of Natural and Applied Sciences of Middle East Technical University, Ankara, Turkey, 2005.
5. Raghunath, N.; Pandey, P.M. Improving accuracy through shrinkage modelling by using Taguchi method in selective laser sintering. *Int. J. Mach. Tools Manuf.* **2007**, *47*, 985–995. [CrossRef]
6. Caulfield, B.; McHugh, P.E.; Lohfeld, S. Dependence of mechanical properties of polyamide components on build parameters in the SLS process. *J. Mater. Process. Technol.* **2007**, *182*, 477–488. [CrossRef]
7. Schmidt, M.; Pohle, D.; Rechtenwald, T. Selective Laser Sintering of PEEK. *Ann. CIRP* **2007**, *56*, 205–208. [CrossRef]
8. Yan, C.; Shi, Y.; Yang, J.; Liu, J. Preparation and selective laser sintering of nylon-12 coated metal powders and post processing. *J. Mater. Process. Technol.* **2009**, *209*, 5785–5792. [CrossRef]
9. Karmiris-Obratański, P.; Papazoglou, E.L.; Karkalos, N.E.; Markopoulos, A.P. Volume energy density and laser power: Key determinants in SLS-processed PA12 mechanical properties. *Int. J. Adv. Manuf. Technol.* **2023**, *130*, 2505–2522. [CrossRef]
10. Pilipović, A. Influence of Processing Parameters on the Properties of Polymer Prototype. Ph.D. Thesis, University of Zagreb Faculty of Mechanical Engineering and Naval Architecture, Zagreb, Croatia, 2012.
11. Senthilkumaran, K.; Pandey, P.M.; Rao, P.V.M. Influence of building strategies on the accuracy of parts in selective laser sintering. *Mater. Des.* **2009**, *30*, 2946–2954. [CrossRef]
12. Berce, P.; Păcurar, R.; Bâlc, N.; Păclişan, D. SLS parameters optimization using the Taguchi method. In Proceedings of the 2nd International Conference on Additive Technologies; DAAAM Specialized Conference, Ptuj, Slovenia, 17–18 September 2008.
13. Stoia, D.I.; Linul, E.; Marsavina, L. Influence of Manufacturing Parameters on Mechanical Properties of Porous Materials by Selective Laser Sintering. *Materials* **2019**, *12*, 871. [CrossRef] [PubMed]
14. El Magri, A.; Bencaid, S.E.; Vanaei, H.R.; Vaudreuil, S. Effects of Laser Power and Hatch Orientation on Final Properties of PA12 Parts Produced by Selective Laser Sintering. *Polymers* **2022**, *14*, 3674. [CrossRef] [PubMed]
15. Wörz, A.; Drummer, D. Understanding hatch-dependent part properties in SLS. In Proceedings of the Solid Freeform Fabrication 2018: Proceedings of the 29th Annual International Solid Freeform Fabrication Symposium—An Additive Manufacturing Conference, Austin, TX, USA, 13–15 August 2018.
16. Lopes, A.C.; Sampaio, A.M.; Pontes, A.J. The influence of the energy density on dimensional, geometric, mechanical and morphological properties of SLS parts produced with single and multiple exposure types. *Prog. Addit. Manuf.* **2022**, *7*, 638–698. [CrossRef]
17. Razaviye, M.K.; Tafti, R.A.; Khajehmohammadi, M. An investigation on mechanical properties of PA12 parts produced by a SLS 3D printer: An experimental approach. *CIRP J. Manuf. Sci. Technol.* **2022**, *38*, 760–768. [CrossRef]
18. *HRN EN ISO 527-1:2019*; Plastics -- Determination of tensile properties—Part 1: General principles (ISO 527-1:2019; EN ISO 527-1:2019). HZN e-Glasilo 10/2019: Zagreb, Croatia, 2019.
19. Rujnić-Sokele, M. Utjecaj parametara razvlačnog puhanja na svojstva PET boca. *Polimeri* **2007**, *28*, 213–292.
20. Matuš, M.; Bechný, V.; Joch, R.; Drbúl, M.; Holubják, J.; Czán, A.; Novák, M.; Šajgalík, M. Geometric Accuracy of Components Manufactured by SLS Technology Regarding the Orientation of the Model during 3D Printing. *Manuf. Technol.* **2023**, *23*, 233–240. [CrossRef]
21. Korycki, A.; Garnier, C.; Nassiet, V.; Sultan, C.T.; Chabert, F. Optimization of Mechanical Properties and Manufacturing Time through Experimental and Statistical Analysis of Process Parameters in Selective Laser Sintering. *Adv. Mater. Sci. Eng.* **2022**, *2022*, 2526281. [CrossRef]
22. Gazzerro, A.; Polini, W.; Sorrentino, L. Investigation on selective laser sintering of PA12: Dimensional accuracy and mechanical performance. *Rapid Prototyp. J.* **2021**, *27*, 1010–1019. [CrossRef]
23. Ruivo, T.; Correia, M.S.; Almeida, H.A.; Amaro, A.M. Mechanical Behaviour of Polyamide 12 Parts Manufactured by SLS Process. In *Additive Manufacturing in Multidisciplinary Cooperation and Production*; Drstvensek, I., Pal, S., Ihan Hren, N., Eds.; Springer Tracts in Additive Manufacturing; Springer: Cham, Switzerland, 2023. [CrossRef]
24. Jevtić, I.; Golubović, Z.; Mladenović, G.; Berto, F.; Sedmak, A.; Milovanović, A.; Milošević, M. Printing orientation influence on tensile strength of PA12 specimens obtained by SLS. *J. Mech. Sci. Technol.* **2023**, *37*, 5549–5554. [CrossRef]